



Impact of anthropogenic and land use pattern change on spatio-temporal variations of groundwater quality in Odisha, India

Susmita Goswami¹ · Abhishek Kumar Rai¹

Received: 21 December 2022 / Accepted: 13 August 2023 / Published online: 31 August 2023
© The Author(s), under exclusive licence to Springer-Verlag GmbH Germany, part of Springer Nature 2023

Abstract

The groundwater physicochemical parameters were studied to understand their spatiotemporal variations and groundwater quality, using the statistical and entropy weights methods. Out of ten parameters that were considered, F⁻, TDS, and Cl⁻ appear to be the major contributors influencing the quality of groundwater. The Principal Component Analysis (PC1, PC2) indicates that the majority of ions are derived from both natural and anthropogenic sources. Studies of saturation indices of gypsum, Halite, dolomite, and calcite indicate that dissolution of these salts also affects groundwater salinization. In coastal areas, a few of the water samples also appear to be contaminated by the mixing of seawater. The entropy weights, which are free from subjective biases were used to estimate the water quality index. The entropy-based water quality index (EWQI) varies from excellent to good quality for the year 2012-13, and appears to degrade after 2015 onwards. For the year 2018-19 and 2021-22, 71.42% and 68.42% of the study areas show excellent water quality, followed by 25.33% and 24.33% (good), 2.54% and 3.54% (average), 0.7% and 3.7% study area shows as poor quality respectively. The groundwater quality, particularly in the western, central, northern, and eastern parts of the region, appears to be average, poor, and very poor in several small patches, respectively. Industrial developments, mining activities, irrigation, changing land use patterns, agricultural activities, and increased anthropogenic activities may be contributing to the degradation of the water quality.

Keywords Entropy-Based Water Quality Index · Land Used Land Cover · Principal Component Analysis · Saturation Index · Groundwater Quality

Introduction

The demand for groundwater has increased substantially during the last few decades for drinking, agriculture, irrigation, and industrial activities (Gleeson et al. 2012). In urban areas, the availability of potable water supply is becoming more problematic due to unplanned development, population explosion, etc. Climate change and fast urbanization are the main cause of water shortages in many parts of the world (Sophocleous 2004). Around 90% of the rural and more than 50% of the urban population get their drinking water supplies from groundwater resources. Recent studies show that

groundwater storage has declined with time (Nair and Indu 2021), which is a matter of concern for long-term groundwater management plans for sustainable development. The unavailability of suitable water may affect the economic growth and development of society. Groundwater aquifers in coastal areas are also prone to seawater intrusion through hydraulically connected faults and lineaments extending toward the sea (Ketabchi and Ataie-Ashtiani 2015). Saline water intrusion caused by excessive groundwater pumping may considerably affect the potable water supply in coastal areas (Werner et al. 2013), up to at least 100km from the coastline where more than 40% population resides. The groundwater quality is also affected by mining, industrial uses, and untreated sewage discharge in urban areas (Gupta 2002; Robson et al. 2006). Furthermore, the population residing in urban areas is more likely to be exposed to various chemical pollutants during their lifetime (Huang et al. 2020). Groundwater pollution has varying impacts and consequences for different land-use land-covers patterns (Gómez et al. 2017). It has been observed that poor quality of drinking water may

Responsible Editor: Xianliang Yi

✉ Abhishek Kumar Rai
abhishek@coral.iitkgp.ac.in

¹ Centre for Ocean, River, Atmosphere and Land Sciences, Indian Institute of Technology Kharagpur, Kharagpur, WB 721302, India

be the primary cause of about 80% of diseases (Mukherjee et al. 2021). Therefore, considering the health hazards and other issues associated with polluted subsurface water, evaluation of groundwater quality is crucial (He and Wu 2019).

The hydrogeochemistry of groundwater has been studied from time to time, but little attempt has been made to understand spatio-temporal variation of groundwater quality (2012 to 2022) in the coastal state of Odisha, India. In this paper, we used Shannon's entropy theory, GIS technique, and statistical analysis to examine various geochemical characteristics of groundwater in Odisha, and impacts of anthropogenic activities and coastal vulnerability. The first objective is to evaluate major controlling factors of groundwater quality by using Shannon's entropy method. Statistical analysis has been used to analyze and understand the relationship between hydrogeochemical parameters that influence groundwater quality. Variations of LULC between 2012 and 2022 have been used to understand the impacts of anthropogenic, and industrial activities on groundwater quality. The analysis and results may provide valuable inputs to the planners and policymakers involved in water resource management for sustainable development.

The water quality index (WQI) is a widely used method to estimate the quality of water for drinking and irrigation purposes (Goswami and Rai 2022). The aggregation techniques of various sub-indices that are used in WQI studies are discussed in detail by Banda and Kumarasamy, 2020. In brief, there are numerous aggregation methods, but the most common are the multiplicative (geometric), and additive (arithmetic) (Sutadian et al. 2016). The additive method is widely used for aggregating sub-indices in a water quality study (Walski and Parker 1974; Stoner 1978). In some aggregations techniques used for WQI, all parameters are assigned a unit weight (Mohebbi et al. 2013), which appears impractical given that different parameters have varying degrees of influence on water quality. As a result, appropriate weights for water quality parameters must be determined and considered in the aggregation of parameters for WQI estimation (Singh et al. 2008). Among the various WQI evaluation standards such as the Bureau of Indian Standards (BIS), World Health Organization (WHO), and Indian Council of Medical Research (ICMR), the BIS standard has been found to be best suited for WQI analysis (Seifi et al. 2020).

For WQI analysis, calculating the weights of parameters is an important step. Several methods are adopted for calculating weights, e.g. based on the relative importance of variables relative weights on a scale of 1 to 5 are assigned (Brown et al. 1972; Tiwari and Manzoor 1988). Similarly, weights are also estimated using Analytical Hierarchy Process (AHP) (Saaty 1980). However, these are subjective methods, and the assigned weights are likely to be biased by expert opinion (Sutadian et al. 2017). However, the weights

estimated using Shannon's entropy technique (Shannon 1948; Hassan and Rai, 2020), are relatively free from such subjective biases. The term entropy refers to the element's unpredictability as well as the assessment of fuzziness in a system. Shannon entropy is based on probability theory and uses relative weights of attributes to calculate the average information provided to the decision-maker (Shannon and Weaver 1947). Therefore, the water quality index estimated using entropy weights (EWQI) is considered better (Li et al. 2010; Chang and Lin 2014; Hasan and Rai 2020).

Salinization, or seawater intrusion, in coastal aquifers, has become a major concern across the world, particularly in areas where freshwater aquifers are hydraulically linked to seawater (Park et al. 2005). The Na^+ vs Cl^- , Na^+/Cl^- molar ratio and Revelle co-efficient has been used preliminary to understand the impact of seawater intrusion in the study area. On the other hand, the mineral saturation index (SI) has been used to understand the degree of equilibrium of different mineral phases that tend to dissolve and precipitate in the groundwater (Li et al. 2010), which helps to assess the degree of coastal aquifer contamination by seawater intrusion. The details of the methodology and results are discussed in the following sections.

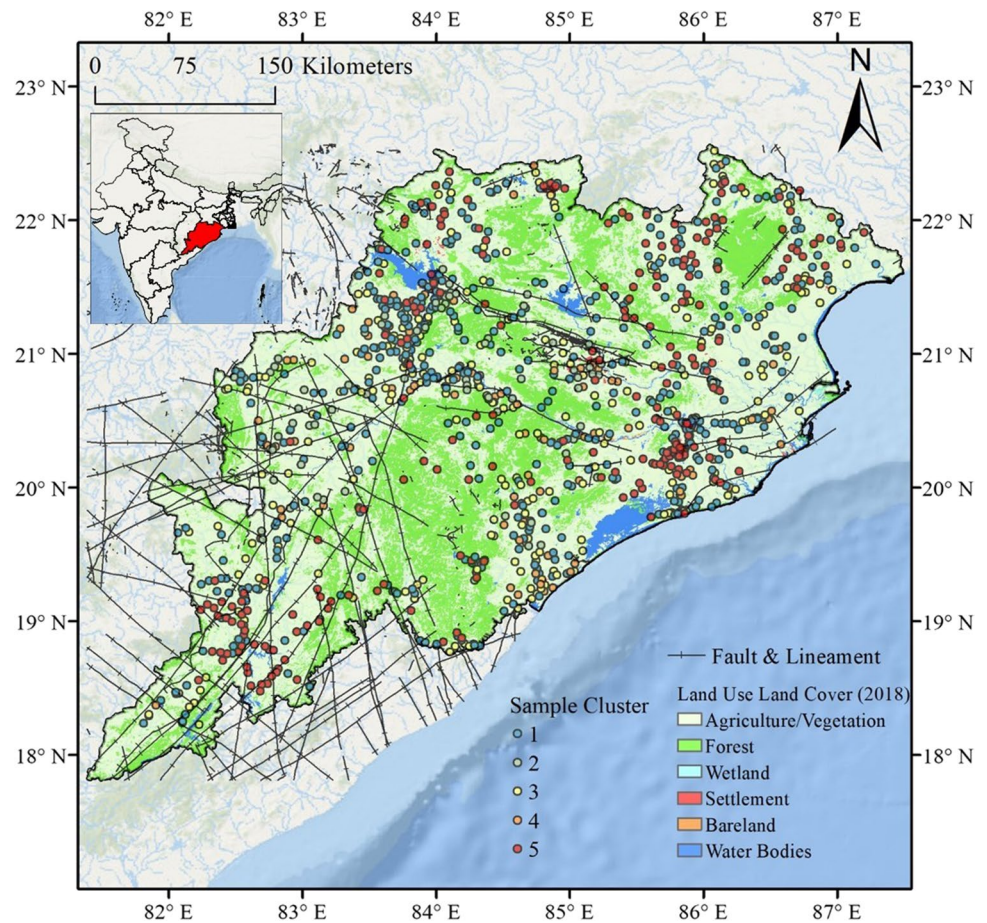
Integrating hydrogeochemical data for understanding groundwater quality with the Geographic Information System (GIS) provides valuable insights into the spatial variability of water quality (Nayak et al. 2017). Several researchers have conducted the hydro-geochemical and groundwater quality study for the region (Das and Anandha Kumar 2005; Shukla et al. 2010; Madhav et al. 2018; Sahu et al. 2021; Goswami and Rai 2022). In this paper, we have attempted to study the spatiotemporal variation of the groundwater quality index, determined using the entropy method, Geospatial, and statistical techniques. We also study the impacts of LULC change, seawater intrusion impacts, and other anthropogenic factors on the water quality in the region. Statistical methods have been used to understand the relationship between various hydrogeochemical parameters influencing groundwater quality. The principal component analysis (PCA) has been used to understand important variables influencing the water quality in the region (Hu et al. 2013; Xiao et al. 2019), whereas attribute-based clustering has been used to identify similar types of water samples. The data, methodology, and results are discussed in the following sections.

Data and Methodology

Study area

The study area is located in the central-eastern part of India (Fig. 1), between latitudes of $17^{\circ}48' - 22^{\circ}34' \text{N}$ and longitudes of $81^{\circ}24' - 87^{\circ}29' \text{E}$. The region can be broadly

Fig. 1 Geographical location of the study area. Sampling locations clustered in 5 groups based on similarity in hydro-geochemical characteristics, are shown by circles of different colours. Major lineaments are shown by black-lines



classified into four zones i.e., the Central River Basin, the Northern Plateau, the Coastal Plains, and the Eastern Ghats Hill Ranges. The granites, granite-gneisses, khondalites, schistose, charnockites, calcsilicates, phyllite, quartzites, shale, marble, sandstone, and limestone rocks are the most common subsurface basement rocks. The Precambrian basement covers 80% of the study region, with ages ranging from Precambrian to Cenozoic. The Mahanadi River Basin occupies around 45%, and the coastal plains account for around 10% of the overall geographical area. The region falls under a tropical climate and is characterized by humid, high temperature, and high to medium rainfall. Annual rainfall varies from 1211–1697mm with an average of 1481mm, where maximum rainfall is observed during the months of July and August, with 85% of rainfall due to the southwest monsoon. The annual temperature varies from ~3 and 6°C in winter, and 45°C during the summer.

The water samples from around 725 sampling locations have been obtained from published reports of various years of the Central Groundwater Board, Govt. of India (CGWB 2012–13, 2015–16, 2018–19, 2021–22). A total of ten groundwater physicochemical parameters have been studied e.g., pH, fluoride (F⁻), calcium (Ca²⁺), magnesium (Mg²⁺), Chloride (Cl⁻), total dissolved solids (TDS),

HCO₃⁻ (bicarbonate), sulfate (SO₄²⁻), TH (total hardness), iron (Fe²⁺). The outlier in the data sets was removed using statistical methods, where data values below the Q1–1.5 IQR or above Q3+1.5 IQR, were identified as the outlier. The Q1 and Q3 are the 25th and 75th percentiles, and IQR is the interquartile range (Q3–Q1). The point data were transformed to raster data by the Inverse distance weighting (IDW) interpolation technique (Watson 1992), and understand the spatial-temporal variation of the several parameters. IDW is a data interpolation method, which is used to evaluate values of data at unsampled locations, using a linear combination of known data from observed locations, using weights that are inversely proportional to the distance of original sampling locations (Watson 1992; Manson et al. 1999). Furthermore, Gibbs's diagram has been used to understand the dominant mechanism that influences the overall groundwater quality in the study region.

Furthermore, to identify broader similarities and differences in the hydrogeochemical composition of the water samples in the study area, the data samples were categorized into clusters based on their composition or attributes. A cluster is a collection of objects aggregated together because of certain similarities. The main aim

of spatial clustering is to partition spatial data into a meaningful subclass called clusters, such that objects in the same cluster have similarities to a great extent, and are dissimilar to those in other clusters. For geo-referenced 2-D spatial data, several spatial clustering algorithms based on attributes have been developed, e.g. partitioning algorithms such as *k*-means (MacQueen 1967) have been applied to solve spatial clustering problems (Miller and Han 2009). K-means clustering is one of the simplest and most popular unsupervised machine learning algorithms. We use k-means algorithms for clustering the hydrogeochemical compositions based on a number of attributes such as pH, TH, and TDS, and categorized the data into five broad categories (Fig. 1).

Correlation Matrix and Principal Component Analysis (PCA)

A correlation matrix study was performed to determine the degree of similarity between different physicochemical parameters. Component matrix analysis has the advantage of classifying the variable data into some organized components, which can be used to draw meaningful inferences. The correlation between the hydrogeochemical groundwater parameters is determined using Pearson's correlation coefficient (*r*) (Ustaoğlu et al. 2020). The correlation coefficient is a useful statistic for illustrating the relationship between dependent and independent variables (Fleury 2005).

Principal Component Analysis (PCA) is another statistical technique used to reduce the dimension of the bulk amount of data and organize it into well-classifiable groups without losing information. PCA was used to identify probable sources of groundwater facies and variables regulating hydrogeochemistry in the study area. Several studies have employed PCA to calculate and identify the primary factors influencing groundwater quality by reducing the dimension of various physicochemical parameters (Williams and Abdi 2010). Principal Components are estimated from the eigenvalue analysis of the correlation coefficient matrix derived from various parameters and were computed using the IBM SPSS Statistics (IBM Corp, 2020) software. The rotated component matrix is the foundation of PCA analyses. Variables with >0.5 rotated loading are considered significant (Sikdar and Chakraborty 2008). PCA illustrates the relationship between primary components influencing the data, and factor loading (Xiao et al. 2019).

Entropy-based Water Quality Index (EWQI)

The following equation has been applied to analyse the entropy, where w_j represents the weights which are functions of entropy (" e_j "). The relative weights are function of

entropy, where smaller weights are associated with higher entropy and vice versa (Shannon 1948).

The entropy of the system is defined as

$$e_j = \frac{1}{\ln(m)} \sum r_{ij} \ln(r_{ij}) \quad (1)$$

Where,

$r_{ij} = \frac{x_{ij}}{\sum_{i=1}^m x_{ij}}$ is the normalized decision matrix (r_{ij}).

Finally, the entropy weights (w_j) are given by

$$w_j = \frac{1 - e_j}{\sum_{j=1}^n (1 - e_j)} \quad (2)$$

Then, the entropy-based water quality index (EWQI) can be represented by (Li et al. 2010)

$$EWQI = \sum_{j=1}^n (w_j \times q_j) = \sum_{j=1}^n \left[\left(\frac{1 - e_j}{\sum_{j=1}^n (1 - e_j)} \right) \times \left(\frac{C_j}{S_j} \times 100 \right) \right] \quad (3)$$

Where " C_j " represents the different physicochemical parameters, and " S_j " indicates the water quality ranking standard as per BIS (2012) values for drinking water. EWQI is considered a better technique than the traditional WQI techniques which are based mostly on subjective weights of different parameters.

Saturation Index (SI)

The mineral saturation index (SI) is used to understand the degree of equilibrium of different mineral phases that tend to dissolve and precipitate in the groundwater (Larson et al. 1942). SI values are calculated using the following equation,

$$SI = \log\left(\frac{IAP}{K}\right) \quad (4)$$

where "IAP" is an ion activity product, and *K* represents the equilibrium constant. A positive SI value ($SI > 1$) suggests the oversaturated condition where minerals will tend to precipitate, whereas a negative value of SI ($SI < 0$) indicates undersaturated conditions i.e., an ongoing mineral dissolution stage. SI value of approximately zero ($SI \sim 0$) indicates an equilibrium condition between water and the mineral (Goswami et al. 2022).

Results and Discussion

Physicochemical Variations

The highest and lowest pH values were observed from 6.5 and 8.59 with a mean value 8.08 and 6.5 to 8.9 with a mean value 7.83 in 2012-13 and 2018-19, respectively (Fig. 2a,

b, c), and vary from slightly acidic to alkaline in nature. While pH in 2021-22 varies from 6.5 to 8.71 and with a mean of 7.83. The highest pH concentration has observed mostly in the western and northeastern parts of Odisha for the year 2012-13 (Fig. 2a). While the spatio-temporal variation between the years 2018-19 pH concentration varies (Fig. 2b). The low pH is caused by acid mine drainage when a significant amount of Fe^{2+} becomes stable

and dissolved in groundwater under reducing conditions (Fig. 2b).

The minimum and maximum concentrations of TDS fall within a range of 37.17 and 1628.85 mg/L with mean value 414.01, 40 and 2766 mg/L with mean value 354.85 mg/L during the period between 2012-13, 2018-19 and 2021-22 respectively (Fig. 2d, e, f). Total Dissolved Particles were calculated

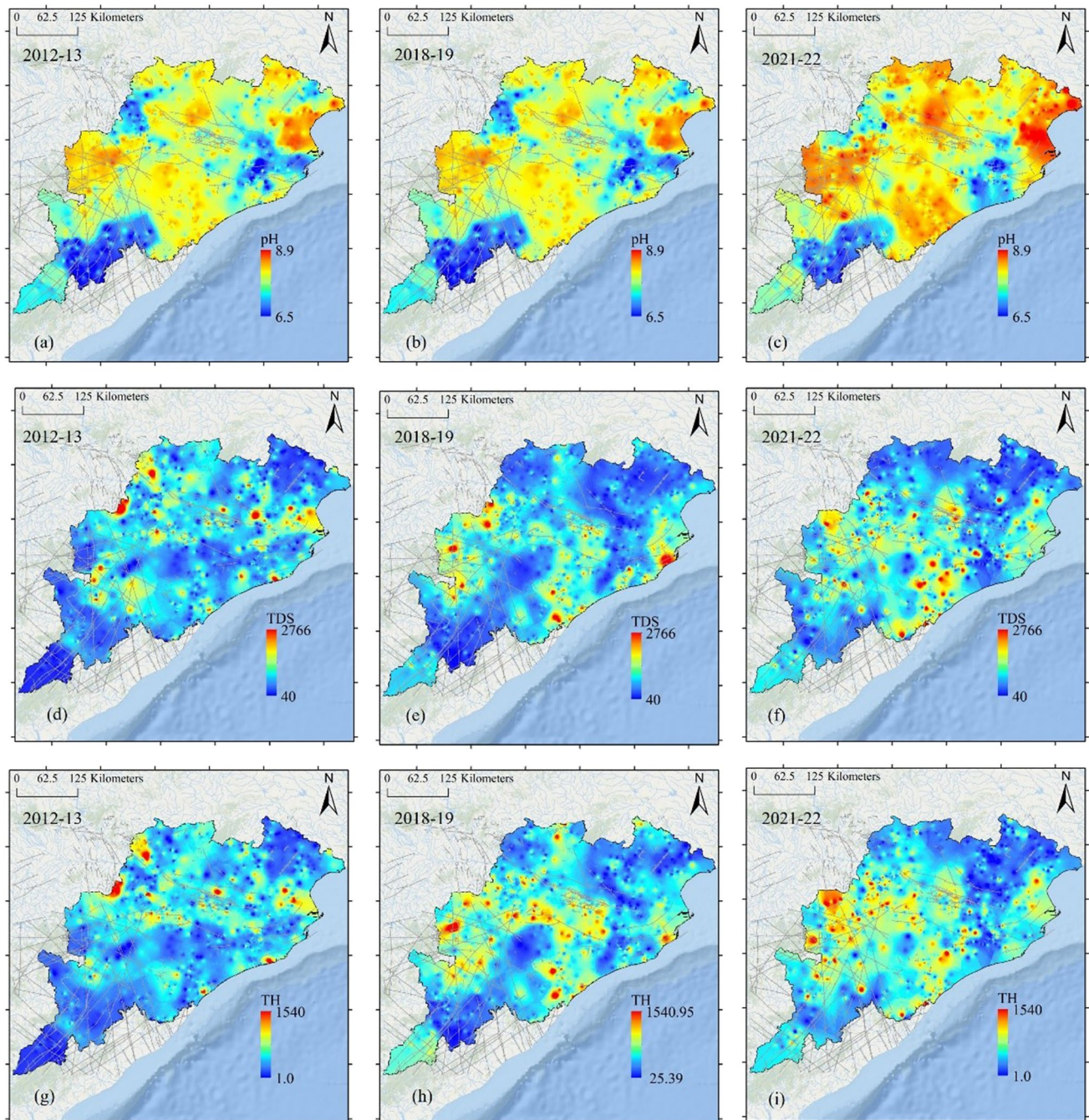


Fig. 2 Spatio-temporal variation of physicochemical parameters i.e. pH (a, b, c), TDS (d, e, f), and TH (g, h, i) during 2012-13, 2018-19 and 2021-22

using the formula $TDS=K*Ec$ (Walton 1989). Because of the mixing of fresh and saline water, and comparatively high EC owing to dissolved ions, the spatial-temporal variation map of TDS values shows a large concentration near the eastern and western parts of the region. Furthermore, because TDS represents the sum of all dissolved ions, the level of groundwater contamination due to anthropogenic activities can be estimated by comparing TDS levels with different ionic types (Rao et al. 2021).

Furthermore, Total Hardness (TH) of groundwater is defined as the amount of multivalent cations in the sample in the presence of alkaline earth (Nag and Das 2017). The higher TH concentration was observed mostly in the western parts of Odisha (Fig. 2g, h, i). The spatio-temporal variation (2018-19) suggests the overall TH concentration has increased (Fig. 2h). The TH values in 2012-13, 2018-19, and 2021-22 vary from 1.0 to 847.79 with mean value of 205.55 mg/L; 25.39 to 1440mg/L with mean value of 210.53 mg/L and 26.39 to 1540 with mean value of 213.59 mg/L in the study area, respectively, indicating that some areas have exceptionally hard water, which can't be used for domestic purpose. According to BIS (2012) standards, the permissible limits are 200mg/l and 600mg/l. Increasing TH in the central to NW parts suggests excessive fertilizer use in the agricultural land, mines, seepage, and runoff from the soil, which percolates and contaminates groundwater quality and increases the hardness in the study region.

The spatial-temporal variations of Ca^{2+} and Mg^{2+} are shown in Fig. 3(a, b, c, d, e, f), and are seen to be increasing between 2012-13, 2018-19, and 2021-22. For the year 2012-13 the Ca^{2+} mostly varies in the eastern and central parts of the study region. The spatio-temporal variations (2018-19) of the Ca^{2+} concentration increase towards the western, Central, and north-western parts of the study area (Fig. 3 a, b). While in 2021-22 the Ca^{2+} ions are seen to be increased towards the western, central, and few eastern parts of Odisha (Fig. 3c).

The highest concentration of Mg^{2+} was observed in the western parts of the study region for the year 2012-13 (Fig. 3d). The spatio-temporal variation (2018-19) of Mg^{2+} concentration is increased along the eastern and western parts of Odisha (Fig. 3e). During 2021-22 the increased of the Mg^{2+} concentration along the western, central parts of the study area (Fig. 3f). The highest HCO_3^- concentration was observed in the central parts for 2012-13 (Fig. 3g). The spatial-temporal variation of HCO_3^- (2018-19) and (2021-22) concentration increased along the eastern, central, and western parts as well (Fig. 3h, i). The highest SO_4^{2-} was observed in the north-western parts for the year 2012-13 (Fig. 4a). The spatio-temporal distribution of SO_4^{2-} concentration is increased towards the eastern and central and western parts of Odisha (Fig. 4b, c). The highest concentration of Cl^- was observed along the western and

northeastern parts for the year 2012-13 (Fig. 4d), whereas the spatial distribution of Cl^- concentration is slightly increased along the eastern and western parts of the study area for the year 2018-19 and 2021-22 respectively (Fig. 4e, f).

The mean of Cl^- concentrations are 97.81, 97.20 and 98.79 mg/L for the year of 2012-13, 2018-19 and 2020-21 respectively. The mean SO_4^{2-} concentration values are 21.52, 25.80, and 25.51 mg/L for the year of 2012-13, 2018-19 and 2020-21 respectively. The mean concentration value of HCO_3^- 154.44 (2012-13), 178.62 (2018-19), and 210.89 (2020-21) mg/L respectively. The mean concentration value of Mg^{2+} 22.75, 25.08, and 25.71 mg/L for the year of 2012-13, 2018-19 and 2020-21 respectively. The mean concentration value of Ca^{2+} 44.84 (2012-13), 42.96 (2018-19), and 44.29 (2020-21) mg/L respectively. The mean concentration of F^- value is 0.45, 0.47, and 0.49 mg/L for the 2012-13, 2018-19 and 2020-21 respectively.

A correlation matrix analysis (Table 1) shows that physicochemical parameters such as Ca^{2+} ($r=0.85$ and $r=0.79$); Mg^{2+} ($r=0.91$ and $r=0.90$); Cl^- ($r=0.80$ and $r=0.82$); and TDS ($r=0.84$ and $r=0.84$) are strongly and positively correlate with TH for the years 2012-13 and 2021-22. TH is weakly correlated with F^- ($r=0.19$ and $r=-0.03$). TDS is positively correlated with Cl^- ($r=0.94$ and $r=0.90$) for 2012-13 and 2021-22, which indicates that groundwater may be influenced by seawater. The TDS and Cl^- values confirmed intermixing of fresh/saltwater in the coastal area through faults and fractures. Whereas Ca^{2+} and SO_4^{2-} correlation ($r=0.56$ and $r=0.42$) for the years 2012-13 and 2021-22 indicates the possible impact of the dissolution of evaporites (gypsum) e.g., $CaSO_4 \cdot 2H_2O = Ca^{2+} + SO_4^{2-} + 2H_2O$.

For 2012-13, only two Principal Components (PC1, PC2) were sufficient to explain most of the variance (73.755%) of the data (Fig. 7a). The first principal component (PC1) consists of TDS, TH, Ca^{2+} , Mg^{2+} , Cl^- , and SO_4^{2-} which are responsible for 58.517% of overall variances data. Similarly, PC2 which is responsible for 15.238% of the overall variance is dominated by pH, F^- , and HCO_3^- . On the other hand, for 2018-19 three principal components (PC1, PC2, PC3) were required to explain most of the variance (74.860%) of the data (Fig. 7b). The first principal component (PC1) comprised TDS, TH, Ca^{2+} , Mg^{2+} , Cl^- , and SO_4^{2-} and explains the overall 52.950% variance. PC2 explains the 12.782 % (2018) total variance consisting of pH, HCO_3^- , and Fe^{2+} PC3 explains the 9.128% (2018) overall variance in the study area and is strongly loaded with F^- . While in 2021-22 the three PCA accounts for 77.783% of the variance in the data set. The first principal component (PC1) comprised of TDS, TH, Ca^{2+} , Mg^{2+} , Cl^- , SO_4^{2-} and explains 52.543% variance in the data. The Second principal component i.e., PC2 comprised of pH and HCO_3^- , Fe^{2+} suggests the 14.77%

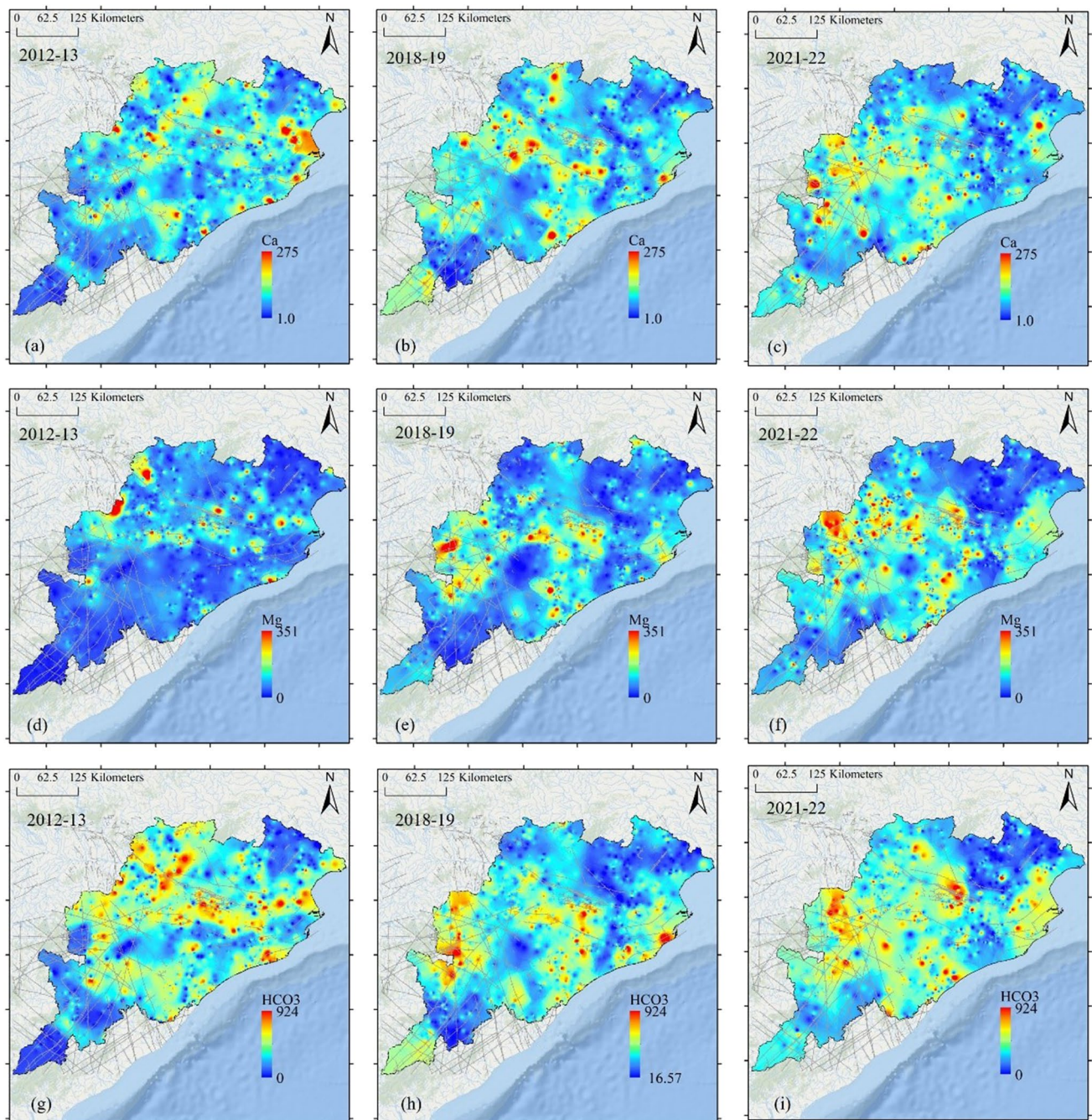


Fig. 3 Spatio-temporal variation of the ions i.e. Ca^{2+} (a, b, c), Mg^{2+} (d, e, f), and HCO_3^- (g, h, i) during 2012-13, 2018-19 and 2021-22

total overall variance of the groundwater quality. The third principal component extracted mainly F^- i.e., PC3 explains the overall 10.470% overall variance of the study area.

Ionic variations

The concentration of Ca^{2+} (Fig. 3a, b, c) in groundwater is influenced by the rock types and sedimentary rock of marine origin, which have a mixture of anhydrite, gypsum,

aragonite, calcite, and dolomite. Calcium in groundwater may be caused by the chemical breakdown of calcic-plagioclase feldspars and pyroxenes (Ganyaglo et al. 2010) or may agricultural fertilizers originate Ca^{2+} from lime (Saha et al. 2019). Ca^{2+} and Mg^{2+} ions are released into groundwater via weathering of dolomite, limestone, anhydrite, and gypsum as well as cation exchange activities (Goswami and Rai 2022). Ca^{2+} and Mg^{2+} concentrations may have been influenced by long-term natural processes

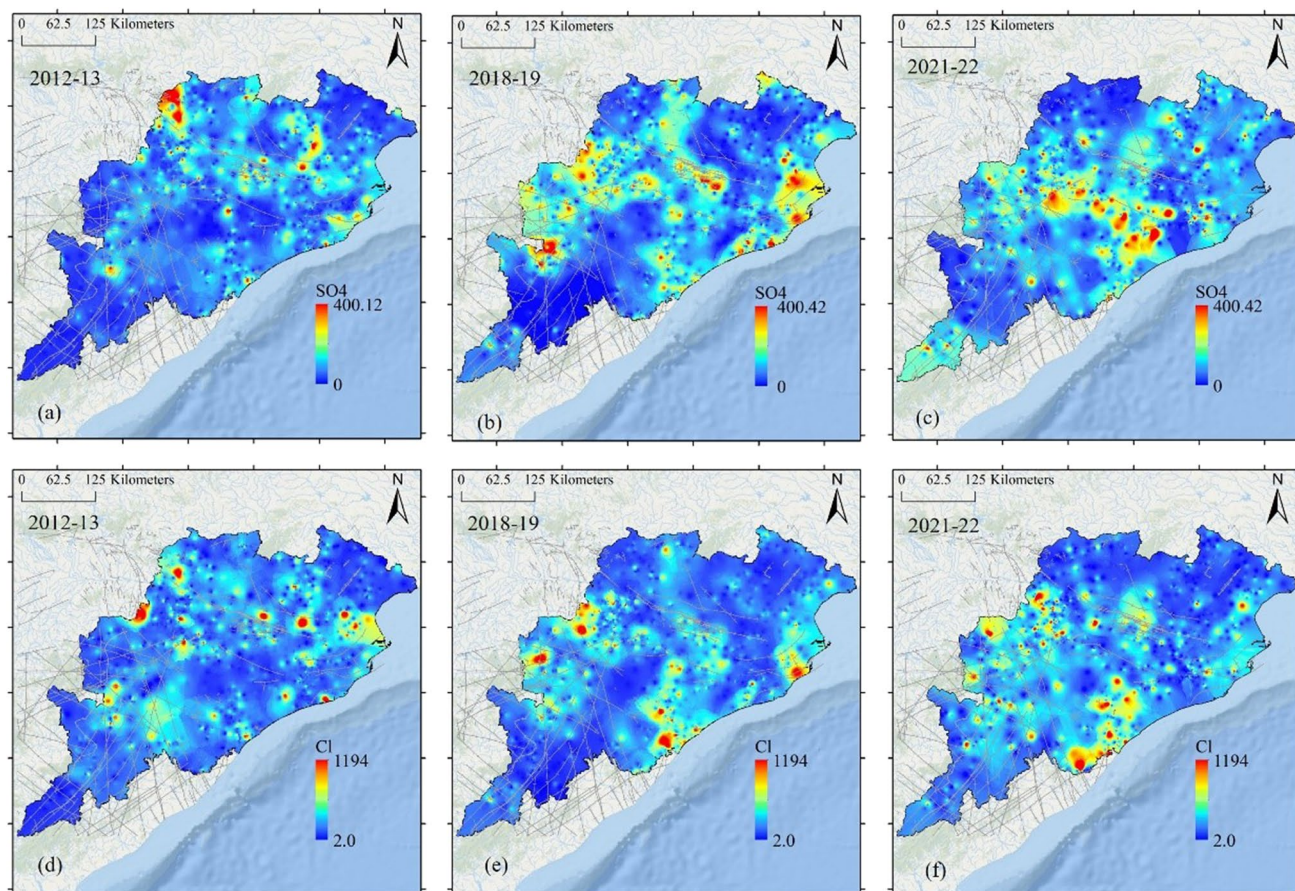


Fig. 4 Spatio-temporal variations of physicochemical parameters: SO_4^{2-} (a, b, c); Cl^- (d, e, f) during 2012-13, 2018-19 and 2021-2

in eastern and western parts of Odisha specifically where concentration shows higher (Fig. 3a, b, c, d, e, f). Anthropogenic activities such as the use of fertilizer, sewage discharge, and animal waste disposal may have contributed to the ionic concentration variability as per LULC variations in the study area. Presumably, an increase in the concentration of Ca^{2+} and Mg^{2+} in the eastern to western parts results from the dissolution of evaporite minerals (anhydrite, gypsum), and sedimentary rocks (dolomites), whereas Mg^{2+} is possibly contributed by anorthosite and albite rock. The excess magnesium is found in groundwater as a result of the disintegration of ferromagnesian rocks such as pyroxene, amphiboles, olivine, and dark-colored micas and domestic wastes or precipitation of Ca^{2+} (Tiwari and Singh 2014).

The correlation between Ca^{2+} , Mg^{2+} , and Th suggests that untreated industrial wastewater may be penetrating and mixing with subsurface water, enhancing the total hardness. Magnesium degrades soil composition by increasing salinity and sodium in water, resulting in

alkaline soil and crop failure (Paliwal 1972). Thapa et al. (2017) also found that high Mg^{2+} concentrations in irrigation water can harm plants due to decreased K^+ in soils. Magnesium hazard (Ragunath, 1987) is given as

$$\text{Magnesium hazard (MH)} = \frac{\text{Mg}^{2+} \times 100}{(\text{Ca}^{2+} + \text{Mg}^{2+})}$$

Here, all parameters are in mg/L. Magnesium Hazard was estimated to determine the consistency of groundwater for irrigation purposes. The calculated MH values ranged from 3.25 to 100, averaging 45.09. Approximately 61% of the groundwater samples appear to be suitable for irrigation, while the other 39% seem hazardous and unsuitable for irrigation ($\text{MH} > 50\%$).

The presence of HCO_3^- indicates the dissolution of carbonate/sedimentary rocks weathering and carbonic acid dissolving in aquifers (Stumm and Morgan 2012; Singh et al. 2012) or maybe silicates-bearing minerals in the study area (Fig. 3g, h, i). Depending on the presence of

Table 1 Pearson's correlation matrix of the hydrogeochemical parameters ($n=725$)

(a) 2012-2013										
Correlation	pH	TH	Ca ²⁺	Mg ²⁺	HCO ₃ ⁻	Cl ⁻	SO ₄ ²⁻	F ⁻	TDS	
pH	1	0.04	0.01	0.06	0.26	0.01	0.03	0.19	0.08	
TH	0.04	1	0.85	0.91	0.54	0.81	0.74	0.19	0.84	
Ca ²⁺	0.01	0.85	1	0.58	0.35	0.68	0.56	0.09	0.67	
Mg ²⁺	0.06	0.91	0.58	1	0.58	0.74	0.74	0.26	0.8	
HCO ₃ ⁻	0.26	0.54	0.35	0.58	1	0.37	0.47	0.47	0.62	
Cl ⁻	0.01	0.81	0.68	0.74	0.37	1	0.7	0.15	0.94	
SO ₄ ²⁻	0.03	0.74	0.56	0.74	0.47	0.7	1	0.22	0.77	
F ⁻	0.19	0.19	0.09	0.26	0.47	0.15	0.22	1	0.25	
TDS	0.08	0.84	0.67	0.8	0.62	0.94	0.77	0.25	1	
(b) 2020-21										
Correlation	pH	TDS	TH	Ca ²⁺	Mg ²⁺	HCO ₃ ⁻	Cl ⁻	SO ₄ ²⁻	F ⁻	Fe ²⁺
pH	1	0.13	0.09	-0.05	0.084	0.272	0.02	0.11	-0.06	0.28
TDS	0.13	1	0.843	0.66	0.77	0.656	0.904	0.672	0.058	0.23
TH	0.09	0.84	1	0.792	0.902	0.514	0.825	0.549	0.031	0.05
Ca ²⁺	-0.05	0.66	0.79	1	0.472	0.322	0.662	0.425	0.002	0.28
Mg ²⁺	0.08	0.77	0.90	0.47	1	0.514	0.744	0.507	0.056	0.42
HCO ₃ ⁻	0.27	0.656	0.514	0.32	0.514	1	0.315	0.409	0.081	0.16
Cl ⁻	0.02	0.904	0.825	0.66	0.744	0.315	1	0.506	0.028	0.25
SO ₄ ²⁻	0.11	0.672	0.549	0.425	0.507	0.409	0.506	1	0.04	0.01
F ⁻	-0.06	0.058	0.031	0.002	0.056	0.081	0.028	0.04	1	0.3
Fe ²⁺	0.28	0.23	0.05	0.28	0.42	0.16	0.25	0.01	0.3	1

dissolved CO₂ and carbonic acid, the carbonate minerals present along the path will be dissolved during infiltration of rainwater and irrigated water ($CO_2 + H_2O = H_2CO_3$). HCO₃⁻ and Ca²⁺ are released into the groundwater during recharge. The Cl/HCO₃ ratio varies between 0.1 and more than 10, suggesting that the Cl⁻ presence in groundwater is caused by irrigation's return flow or natural salt dissolution (Luszczynski and Swarzenski 1996). Chloride is the major seawater ion but occurs in much lower concentrations in groundwater. While HCO₃⁻ is the most common anion in groundwater but occurs in low concentrations in marine water. Therefore, the Cl/HCO₃ anions ratio is used to measure the degree of seawater contamination of freshwater aquifers. Our study indicates that 55.17% of groundwater samples were of good quality, whereas 37.14% were relatively less contaminated, and 7.58% of samples were moderate to highly contaminated (Table 5).

The presence of SO₄²⁻ in subsurface water suggests exposure to soluble sulfate-bearing minerals/evaporate rocks and anthropogenic activities in the region. High SO₄²⁻ may also result from chemical fertilizers used in irrigation and industrial wastewater in the study region. It is observed that SO₄²⁻ and Cl⁻ (Fig. 4) show a mean value (>126 mg/L) above the permissible limit (BIS, 2012), which may be due to sulphur gases released by industry and utilities are oxidized and contaminating the groundwater. The major anions SO₄²⁻ are rapidly depleted in the

coastal aquifer due to seawater intrusion (De Montety et al. 2008). For halite (Na⁺Cl⁻), and gypsum (Ca²⁺SO₄²⁻·2H₂O) indicates that the continued mineral dissolving process is leading to salinization.

The presence of more Cl⁻ in the groundwater near coastal areas suggests infiltration of seawater, which raises the salinity. The chloride concentration in drinking water should not exceed 250mg/l (0.25 g/l) according to WHO guidelines (Manh et al. 2014). Chlorine can cause dry, itchy skin, stomach aches, vomiting, and diarrhea. The western parts show higher Cl⁻ concentrations probably due to contaminations of industrial wastewater or domestic sewage, inorganic fertilizer, decomposition and dissolution of decomposition of organic matter, effluent from septic tanks, discharge of domestic trash, and industrial wastewater near the industrial area (Appelo and Postma 1996; Kelly 2008). While eastern parts (Fig. 4d) show higher concentration due to excessive penetration of seawater in the study regions via faults and fracture (Goswami et al. 2022).

The excess F⁻ (>1.0mg/L) was also observed in the study area, and are shown by a red circle (Fig. 5a). The Excess of fluoride in groundwater is a major threat, and can cause dental, skeletal, and non-skeletal fluorosis and other health problems. The higher F⁻ concentrations are mostly due to the weathered of fluoride-bearing minerals/rocks (fluorite, apatite, topaz, muscovite, cryolite) (Hem 1989; Goswami and Rai 2022). Apart from geogenic factors, F⁻ may also be

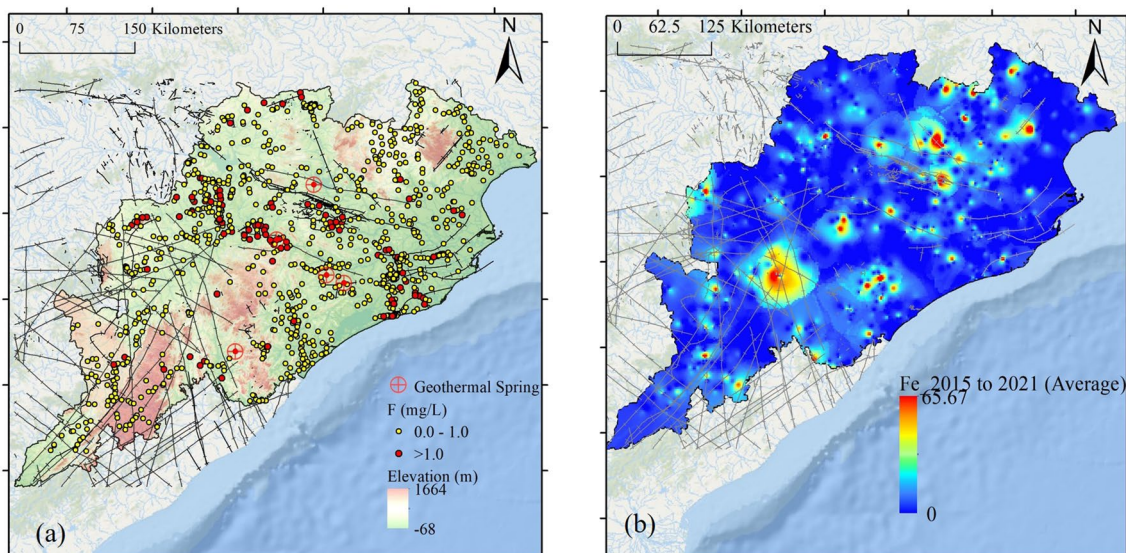


Fig. 5 (a) Spatio-temporal variation of F^- concentration, the red cross circle represents the hot spring; (b) Spatial distribution of average Fe^{2+} Iron concentration in the region

contributed due to anthropogenic activities such as the burning of coal, extraction of aluminium and steel, and fertilizer industry particularly phosphate in areas such as Sambalpur and the Bargarh districts which are in the western parts. High concentrations particularly in some geothermal regions such as Khurda, Anugul, and Nayagarh districts may be due to the presence of Hot-springs and their interactions with the subsurface water (Kundu et al. 2001).

The Fe^{2+} concentration has varied from 0 to 65.67 mg/L between the 2015–2018 years, which exceeds the permissible limit (Fig. 5b). Ferric iron (Fe^{3+}) rapidly precipitates as iron oxide (Fe_2O_3), iron hydroxide ($Fe(OH)_2$), or poorly crystalline to amorphous material at normal groundwater pH values. Ferrous iron is stable under reduced conditions and will remain dissolved in groundwater. Naicker et al. (2003) discovered that oxidation of pyrite (FeS_2) present in mine tailing dumps polluted and acidified groundwater inside the mining district. Acidic groundwater is corrosive; thus, it dissolves iron and increases its concentration when it flows through pipes, pumps, and other equipment. The maximum chromite and iron mines are situated in Odisha's northwest and western parts. The Fe^{2+} concentration increased between 2015–16; which signifies that the rapidly increasing mining industry relies heavily on iron and chromite ore. However, if too much Fe^{2+} is present in water, it creates red oxyhydroxide precipitates that stain clothing and plumbing fixtures, making it an unwanted pollutant in home and industrial wastewater sources. Some of the important Fe^{2+} belts in the study area include Jamda-Koira Belt (Fe), Bonai-Badampahar Belt (Fe), Noamundi-Jamda Belt (Mn, Fe), East Coast Province (Al), Garumahasani Province (Fe),

etc. As per the BIS standard limit of Fe^{2+} concentration in groundwater is 0.3mg/L, the excess amount of Fe^{2+} shown in the map (Fig. 5b) in the northern and south-western parts of Odisha due to excess Fe^{2+} mining industries located and water starts degrading. From 2012 onwards, the iron concentration increased and deteriorated the groundwater quality. Furthermore, a recent study has been done by Ranjan et al., 2020, which suggested that the mining activity become a serious threat to forest resources of the Jharsuguda district of Odisha between 2006–2016.

The saturation index analyses (Fig. 6) show that precipitation and dissolution of aragonite, calcite, Halite, anhydrite, dolomite, and gypsum mineral assemblages play a significant role in contributing HCO_3^- , Ca^{2+} , SO_4^{2-} , Mg^{2+} , and Cl^- . The samples appear to be oversaturated ($SI > 0$) with respect to aragonite, calcite, and dolomite mineral assemblages and undersaturated with respect to Halite, anhydrite, and gypsum (Fig. 6a). The bi-variate SI plots for Halite, gypsum, and anhydrite shows a positive correlation with SO_4^{2-} , whereas calcite, dolomite, and aragonite show a very weak to marginal negative correlation with SO_4^{2-} (Fig. 6b, c, d).

The analysis of the first principal component (PC1) for the year 2012–13 (Table 2a; Fig. 7a) represents that the region is influenced by a natural process such as seawater intrusion, dissolutions of evaporate minerals, water-rock interaction, cation exchange, household wastewater, etc. The second component i.e., PC2 suggests an association of bicarbonates with F^- in groundwater (Table 2a), which may be related to groundwater recharge. This also indicates that groundwater may have been deteriorating due to weathering of geogenic rocks, interaction with fluoride-bearing

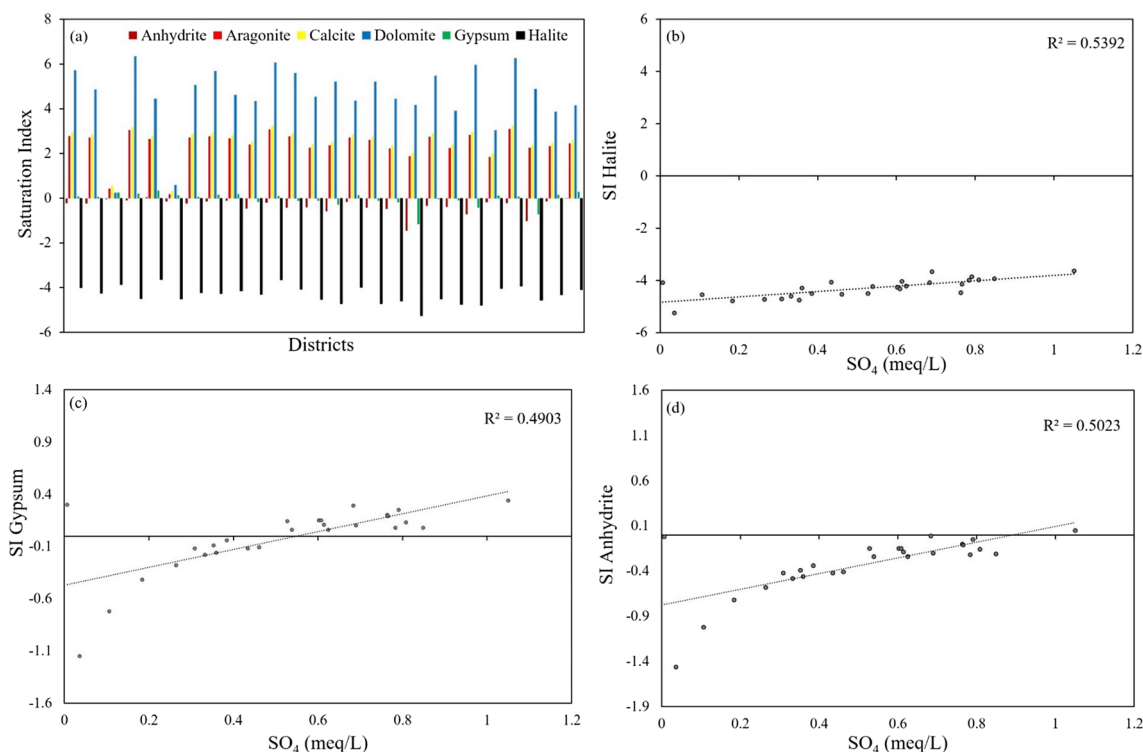


Fig. 6 a Mineral saturation index indicating precipitation and dissolution of mineral assemblages, (b, c, d) variations of SI of Halite, Gypsum and Anhydrite w.r.t. SO_4^{2-}

minerals/rocks or anthropogenic activities or interaction with Hot-springs water.

PC1 for the year 2018-19 and 2021-22 indicates a strong influence of natural processes such as saline water intrusion, dissolutions of evaporate minerals, water-rock interaction, cation exchange (Table 2b, Fig. 7b). PC2 explains the overall variance may be due to anthropogenic activities, fertilizers, irrigations, pesticides, mining development, and mineral explorations (mining industrial swages, untreated mining wastages, wastewater, etc). The HCO_3^- is derived from the geogenic sources and detailed explanations given in reports (Goswami and Rai 2022). In recent years, groundwater quality in the Odisha districts of Jajpur, Keonjhar, Sundargarh, Dhenkanal, and Nuapada has worsened due to heavy contamination from iron (Fe^{2+}) and chromite mining wastes. The third principal component (PC3) suggests the groundwater quality deteriorates due to geogenic factors of weathering of fluoride-bearing minerals/rocks or anthropogenic activity.

The Gibbs diagram (Gibbs 1970) is divided into three distinct fields, i.e. water-rock interaction, evaporation, and precipitation dominance field on the basis of cations $[(\text{Na}+\text{K})/(\text{Na}+\text{K}+\text{Ca})]$ and anions $[\text{Cl}/(\text{Cl}+\text{HCO}_3^-)]$ concentration against the TDS (Fig. 8). Chemical weathering, evaporation-crystallizations, and ionic exchange are the major dominant the geochemical processes that affect groundwater chemistry

and regional geology of the study area. The groundwater samples broadly fall within the water-rock interaction and evaporation dominance field. The evaporation zone also illustrates that marine saline water or the dissolution of evaporation-bearing minerals can have an effect on the regions (Halite). As a result, PC1 which contributes to the dominant ions in the study area, may be due to the natural hydrogeochemical environment in all the years under consideration.

Entropy-Based Water Quality Index (EWQI)

The entropy weights estimated for the anions such as F^- ($w_j=0.235$), TDS ($w_j=0.157$), Cl^- ($w_j=0.156$), and SO_4^{2-} ($w_j=0.128$) indicate that these ions have more influence out of the ten parameters that were considered in this study, as they have the highest entropy weights (Table 3). The weights for Ca^{2+} and Mg^{2+} are 0.055 and 0.059 respectively, and are less than 0.10, indicating that these cations have a minor influence on the overall groundwater quality. The weight for pH was found to be 0, indicating that pH may not contribute much to the groundwater quality variations. The hydrogeochemical parameters sorted based on their relative weights and impact on groundwater quality can be arranged in sequence $\text{F}^- > \text{TDS} > \text{Cl}^- > \text{SO}_4^{2-} > \text{Fe}^{2+} > \text{Mg}^{2+} > \text{TH} > \text{Ca}^{2+} > \text{HCO}_3^- > \text{pH}$ in a decreasing order for the year 2018-19 and 2021-22 respectively. Thus, as per the entropy calculation, five

Table 2 Principal component analysis for groundwater sample

(a) 2012-13			
Rotated Component Matrix			
Parameter (2012-13)	PC1	PC2	
pH	-0.081	0.691	
TH	0.956	0.117	
Ca ²⁺	0.821	-0.035	
Mg ²⁺	0.874	0.226	
HCO ₃ ⁻	0.498	0.677	
Cl ⁻	0.909	0.02	
SO ₄ ²⁻	0.829	0.151	
F ⁻	0.129	0.76	
TDS	0.924	0.214	
(b) 2021-22			
Rotated Component Matrix			
Parameter (2021-22)	PC1	PC2	PC3
pH	-0.046	0.888	-0.113
TH	0.953	0.102	0.006
Ca ²⁺	0.804	-0.139	-0.063
Mg ²⁺	0.844	0.175	0.072
HCO ₃ ⁻	0.507	0.602	0.187
Cl ⁻	0.908	-0.036	-0.015
SO ₄ ²⁻	0.653	0.248	0.069
F ⁻	0.01	-0.036	0.983
TDS	0.928	0.236	0.071
Fe ²⁺	0.135	0.79	0.074

physicochemical parameters F⁻, Cl⁻, TDS, SO₄²⁻, and Fe²⁺ have most impact the groundwater quality.

Water quality in the region can be categorized into five sets i.e. excellent to good water quality based on the EWQI values for the year 2012-13 (Fig. 9a). EWQI of less than 50 suggests excellent (rank 1) water type, for 50<EWQI<100 the water quality can be considered good quality (rank 2), whereas 100<EWQI<150 indicates average water quality (rank 3). A water quality index between 150 and 200 indicates poor water quality (rank 4), whereas a WQI of

more than 200 suggests inferior water quality (rank 5) (Goswami and Rai 2022). In some areas, the EWQI is less than 100, which is suitable for drinking and cooking (Gao et al. 2020). An EWQI of 100 or more poses risk to human health and may be inappropriate for household use.

For 2012-13, the overall water quality was excellent to good, while in 2015-16 to 2021-22 water quality may have been degraded due to the infiltration of contaminants derived from industrial, mining, household, and fertilizers wastewater discharges. Most of the groundwater samples fall within ranks 1 and 2, i.e., excellent to good quality. On the other hand, relatively average, poor, and very poor groundwater quality shows in small patches in the study area (shown in yellow, orange, and red colour in Fig. 9c; i.e., ranks 3, 4, and 5 appear to be concentrated in the west, central, northern and eastern parts of Odisha (Fig. 9c). Approx. 98% study area shows excellent water quality (rank 1), whereas ~2% shows good water quality (rank 2) in 2012-13 (Fig. 9a). While in 2015-16, ~87.94% study area shows excellent water quality followed by good (11.77% area), average (0.26% area), poor (0.021% area), and very poor (0.005% area) water quality (Fig. 9b). For 2018-19, 71.42% of the study areas show excellent water quality followed by 25.33% (good), 2.54% (average), 0.58% (poor), and 0.12% (very poor) respectively (Fig. 9c). In the year of 2021-22, 42% study area shows the excellent water quality, good (24.33% area), average (3.54% area), poor (2.58% area) and very poor (1.12% area) respectively (Fig. 9d).

The majority of urban and rural settlements are concentrated in fairly small areas (0.31 percent) around major cities. Growing population density along the coast may also be a significant factor in the deterioration of groundwater quality in north-eastern and eastern parts (Fig. 10c). Some of the important mining areas are located in the northern parts of Odisha, such as South Kaliapani, Daitari, Sukrangi, Kaliapani-Block in Jajpur district; Banspani, Khandbandh, B.P.J., Mahaparbat, Sakradihi-Dubna, Bangur, Seremda-Bhadra-sahi, Dalki, Baniapank Gandhamardan block in Keonjhar district and Gorumahisani, Badampahar and Suleipat in

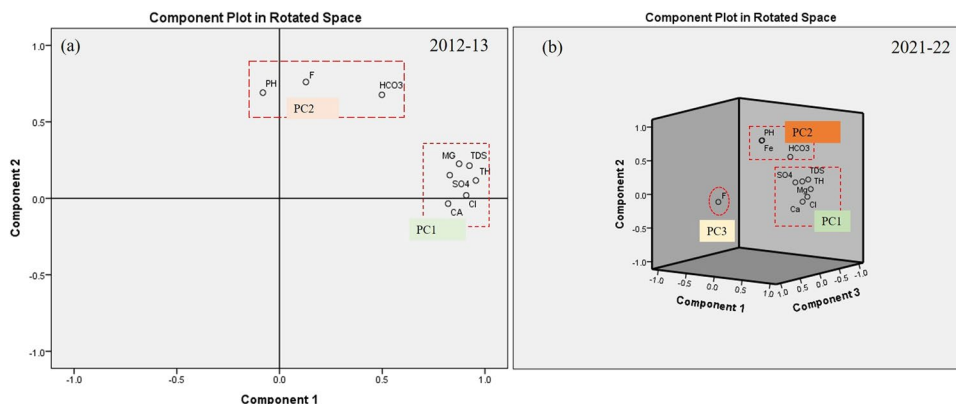
Fig. 7 Principal Component Analysis (PCA) of the groundwater samples

Fig. 8 Gibs Plot showing major processes controlling groundwater geochemistry for the year 2021-2022

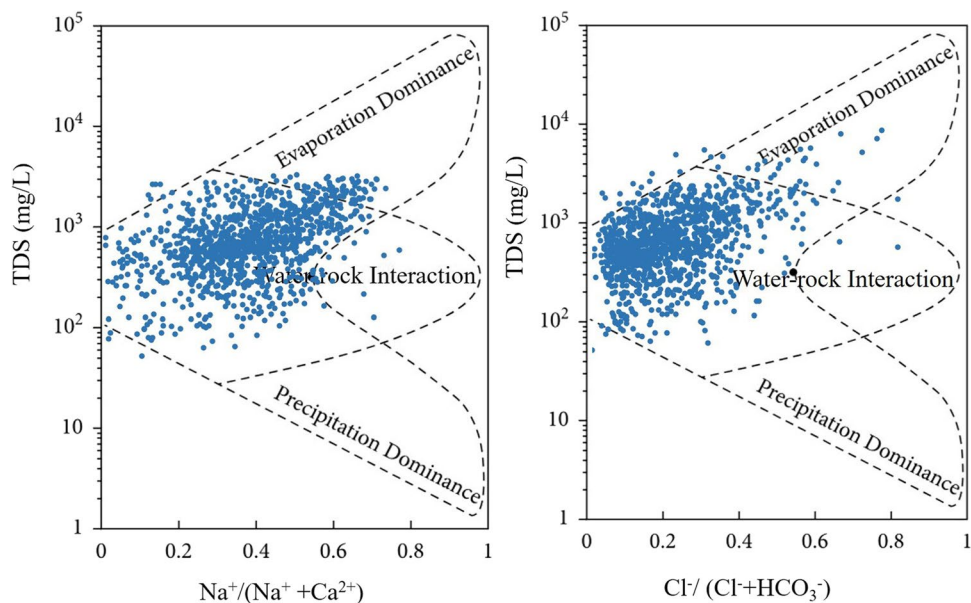


Table 3 The estimates of the entropy (e_j), and the corresponding weights (w_j) for the year (a) 2012-13; (b) 2018-19, by Shannon’s entropy method

(a) 2012-13										
Parameter	pH	TH	Ca ²⁺	Mg ²⁺	HCO ₃ ⁻	Cl ⁻	SO ₄ ²⁻	F ⁻	TDS	
Sum	-0.817	-1.640	-1.454	-1.769	-1.143	-2.014	-1.892	-0.920	-1.549	
e_j	0.124	0.249	0.221	0.269	0.174	0.306	0.288	0.140	0.235	
d_j	0.876	0.751	0.779	0.731	0.826	0.694	0.712	0.860	0.765	
w_j	0.125	0.107	0.111	0.105	0.118	0.099	0.102	0.123	0.109	
(b) 2021-22										
Parameter	pH	TH	Ca ²⁺	Mg ²⁺	HCO ₃ ⁻	Cl ⁻	SO ₄ ²⁻	F ⁻	TDS	Fe ²⁺
Sum	-7.037	-6.834	-6.849	-6.834	-6.877	-6.499	-6.595	-6.227	-6.496	-6.678
e_j	1	0.971	0.973	0.971	0.977	0.923	0.937	0.885	0.923	0.949
d_j	0	0.029	0.027	0.029	0.023	0.077	0.063	0.115	0.077	0.051
w_j	0	0.059	0.055	0.059	0.047	0.156	0.128	0.235	0.157	0.104

Mayurbhanj district. In the western parts of Odisha major mines are located Budhapara block in the Nuapada district. While the north-western parts of Odisha, the major mines are Koira-Bhanjpali, Koira-Kasira, Rantha, and Kumritar located in the Sundargarh district. Most of the mines in the eastern parts are located in the Rayagada district and Dhenkanal district as per the Odisha Mines Corporation (OMC). Other major mining belts are located in the western, north-western, and western parts of Odisha (Fig. 9c), such as the Baula-Nausahi Belt (Cr), Sukinda- Nausahi Belt (Cr), Adash Raimal Belt (Cu), Sukinda Belt (Cr), etc. All these factors may have influenced the subsurface water quality in the study region.

Land Use Land Cover Change

The LULC map (Fig. 10a, b) indicates that the main LULC types are agriculture and vegetation, Forest, wetland,

settlement area, bare land, and water. Further analysis indicates that the area under agricultural and sparse vegetation has decreased from ~68.42% to 66.62 % and from 1.41 to 1.31 between the years 2012 and 2021 respectively. The settlement area has increased from 0.29% to 1.20%, which signifies that urbanization may have increased between 2012 to 2021 respectively (Table 4; Fig. 10a, b). The forest area has changed slightly from 26.20% to 26.96% i.e., 0.76% in the year 2021 (Fig. 10b). Minor increase in forest area, enable holding water, percolation and recharge processes which could slightly improve groundwater water quality in the region. The bare land and wetland area remained unchanged during this period (2012 and 2021). The area of water bodies has increased from 2.68% to 2.78% in the year 2021. These changes will likely impact water quality, general environmental conditions, agricultural productivity, industries, and socioeconomic conditions of society. The settlement area has grown slightly, indicating that anthropogenic activities

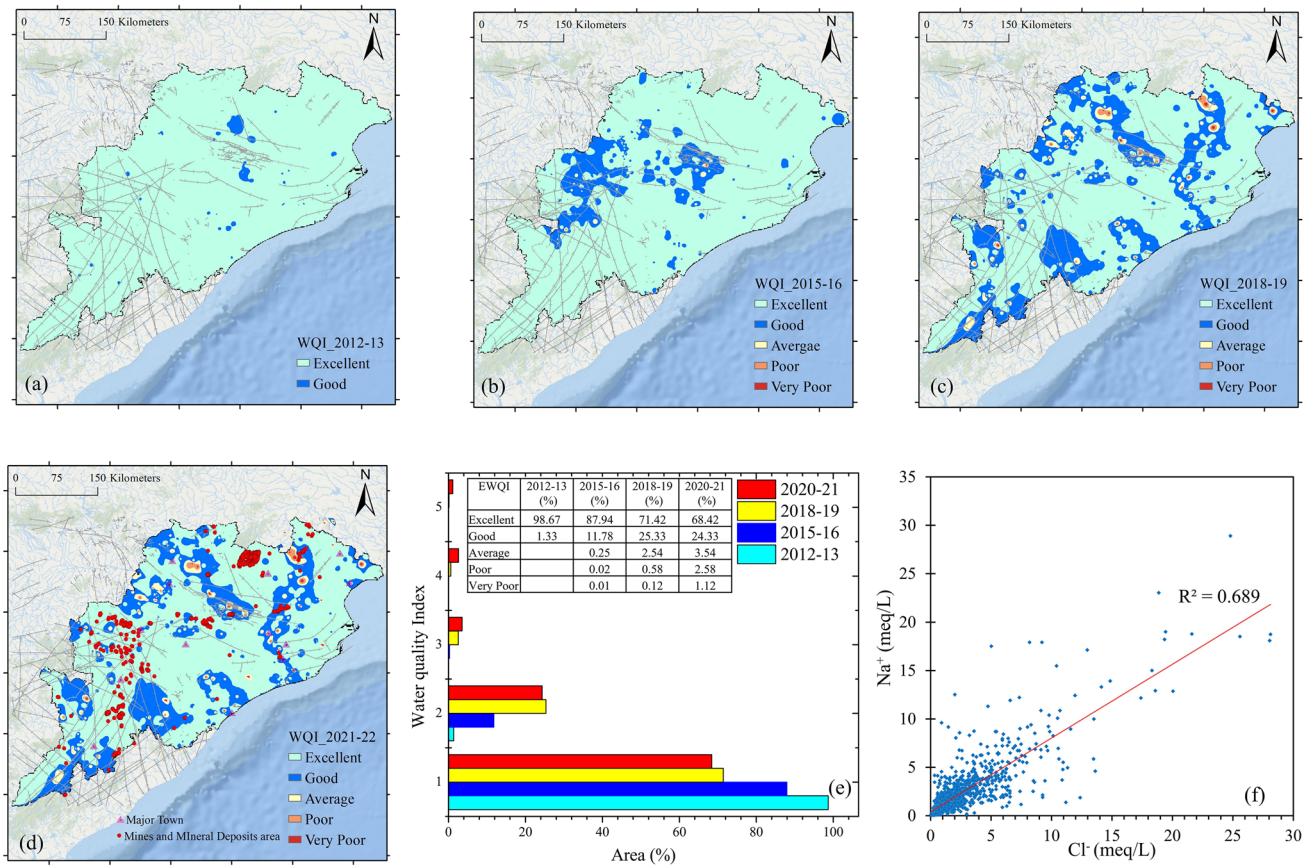


Fig. 9 a, b, c The Spatio-temporal variation of the groundwater quality during 2012-13; 2015-16; 2018-19; 2021-22 (c) Location of urban, Industrial, and major mining and mineral deposits areas are shown in by pink triangle (major town), yellow Circles and stars; (d) The water quality index (WQI) plotted rank with respect to the area (%); (e) Bivariate plot of Na⁺ vs Cl⁻

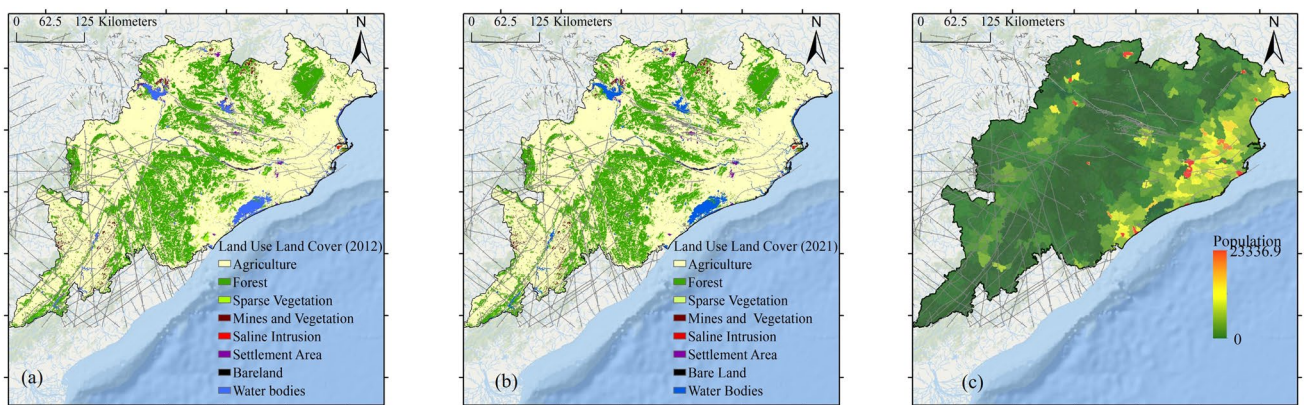


Fig. 10 Land use and Land cover variations during the years (a) 2012, (b) 2021, and (c) Population distribution map of Odisha, and Spatial distribution point of the estimated

may affect the overall groundwater quality between 2012 to 2021 (Fig. 10a, b). The saline intrusion has increased with time from 0.04% to 0.10% between 2012 to 2021. The poor water quality in the eastern parts of may be due to the

intrusion of saline water shown in Fig 9(e). The population density map (Fig. 10c) also suggests that the groundwater quality may deteriorate due to the excess withdrawal and enhanced seawater intrusions during the last few decades.

Table 4 Land Use Land Cover variation from 2012-2018 (ESA 2017)

Year	2012	2021	(2012 - 2021)
LULC	Percentage (%)	Percentage (%)	Change (%)
Agriculture	68.42	66.62	-1.8
Forest	26.2	26.96	0.76
Sparse vegetation	1.41	1.31	0.1
Mines	0.92	0.98	0.06
Saline intrusion	0.04	0.1	0.06
Settlement Area	0.29	1.2	0.91
Bare Land	0.05	0.05	0
Water bodies	2.68	2.78	0.11

Table 5 Classification of the Groundwater Quality based on Revelle Coefficient ($Cl/(CO_3+HCO_3)$)

Classification	Revelle Coefficient	Number of Samples	Samples (%)
Good Quality	<0.5	400	55.17
Slightly Contaminated	0.5-1.3	270	37.24
Moderately Contaminated	1.3-2.8	46	6.34
Highly Contaminated	2.8-6.6	4	0.55
Extremely Contaminated	>6.6	5	0.69

A recent study has been done by Ranjan et al., 2020, which suggested that the mining activity become a serious threat to forest resources of the Jharsuguda district of Odisha between 2006-2016.

Seawater Intrusion

The molar ratio of Na^+/Cl^- is significant in terms of onshore encroachment of seawater; the ratio of 0.86 represents the seawater intrusion, while a ratio of >1.0 freshwater source (Ekhmaj et al. 2014). The Na^+/Cl^- molar ratio of groundwater samples varied from 0.058 to 6.96, with an average of 1.09. Based on a theoretical mixing line, seawater intrusion or evaporite dissolution in the coastal aquifer is indicated by a few samples lying on or near the mixing line in the Na^+ and Cl^- plots (Fig. 9d). The Cl^- concentration appears to be slightly higher than the standard limit (WHO 2017). The correlation coefficient of the Na^+ vs Cl^- plot shows 0.689, suggesting that the study regions may be influenced by seawater intrusion (Fig. 9d).

The Revelle coefficient is the ratio of Chloride and bicarbonate ($Cl/(CO_3+HCO_3)$) and is used to assess the saltwater intrusion in groundwater aquifers (Lobo-Ferreira et al. 2005). Chloride is the major seawater ion but occurs in much

lower groundwater concentrations. While HCO_3^- is the most common anion in groundwater but occurs in low concentrations in marine water. The Cl/HCO_3 anions ratio is used to measure the degree of seawater contamination of freshwater. In the study area, 55.17% of groundwater samples were of good quality, whereas 37.14 percent were relatively less contaminated, and 7.58 percent were moderate to highly contaminated (Table 5).

Conclusions

In this paper, we investigated the groundwater physico-chemical parameters to understand the spatio-temporal variations of various parameters that control the water quality in the region. The uneven distribution of cations in groundwater suggests that the groundwater aquifers have heterogeneous geochemical characteristics. PCA analysis indicates that the region is mainly affected by water-rock or geogenic seawater intrusion/cation exchange process or maybe dissolutions of evaporate minerals, fertilizers, and mining activity. The Principal Component Analysis (PCA) indicates two major principal components PC1 (TDS, TH, Ca^{2+} , Mg^{2+} , Cl^- , and SO_4^{2-} with 45.87% variance), and PC2 (HCO_3^- , and Fe^{2+} with 18.14% variance). This suggests that water may have been influenced by both natural and anthropogenic sources in the study area. For 2021-22, PC1 accounts for 52.543% of data variance and indicates that most ions are derived from natural sources. From the year 2015-16 onward, the Fe^{2+} concentration shows an increasing trend, suggesting that mining activity may have some influence in the region. Furthermore, the saturation index of the dissolution of gypsum, Halite, dolomite, and calcite signifies that the dissolution of these minerals also affected groundwater salinization. Approximately 61% of the groundwater samples were found suitable for irrigation, while the remaining 39% may be unsuitable for irrigation (MH >50%). Shannon's entropy method was used to compute the Entropy-based Water Quality Index (EWQI). The highest entropy weights (0.235, 0.157, 0.156) were found for F^- , TDS, and Cl^- , whereas pH shows relatively lower entropy weight. The EWQI suggests that quality of groundwater in the study region varies from excellent to medium quality. The analysis also indicates that water quality may have been slightly degraded since 2015 due to anthropogenic activities such as industries, mining, and/or agricultural activities, etc. An increase in the settlement area, as seen in the region may also influence the overall quality of subsurface water. The analysis and results may be used for planning and policy decisions by the state pollution control, and water resource management agencies for sustainable development in the region.

Acknowledgments The authors thank the Ministry of Earth Sciences (MoES/PO/(Geo)/90/2017) Govt. of India, and the Indian Institute of Technology Kharagpur for providing funding for the research and required infrastructure. The authors also sincerely thank the CGWB and other agencies for providing the data used. We profoundly thank the editor, and the anonymous reviewers for their constructive comments, which significantly enhanced the quality of the manuscript.

Author Contributions Susmita Goswami: Methodology; Formal analysis; Investigation; Visualization; Writing - original draft.

Abhishek Kumar Rai: Supervision; Conceptualization; Resources; Writing - Review & Editing.

Funding Funding from Ministry of Earth Sciences, Govt. of India was available through its grant number (MoES/P.O.(Geo)/90/2017).

Data availability The data used in this manuscript are publically and freely available.

Declarations

Competing Interests The authors have no relevant financial or non-financial interests to disclose.

Ethics Approval We confirm that this work is original and has not been published elsewhere, nor is it currently under consideration for publication elsewhere.

Consent to participate and publication The authors are willingly participating in publication of this manuscript and give their consent for publication.

References

- Appelo CAJ, Postma D (1996) *Geochemistry, groundwater and pollution*; AA Balkema Publ., USA
- Banda TD, Kumarasamy M (2020) Development of a Universal Water Quality Index (UWQI) for South African River Catchments. *Water* 12:1534. <https://doi.org/10.3390/w12061534>
- Brown RM, McClelland NJ, Deininger RA, O'Connor MF (1972) A water quality index—crossing the psychological barrier. In: *Proceedings of the International Conference on Water Pollution Research*, Jerusalem, 18–24 June 1972, pp. 787–797
- Bureau of Indian Standards (BIS) (2012) Indian standard drinking water specification (Second Revision) BIS 10500:2012, New Delhi
- CGWB (2012–13) Central Ground Water Board Ministry of Water Resources Government of India, Report
- CGWB (2018–19) Central Ground Water Board Ministry of Water Resources Government of India, Report
- CGWB (2020–21) Central Ground Water Board Ministry of Water Resources Government of India, Report
- Chang CL, Lin YT (2014) Using the VIKOR method to evaluate the design of a water quality monitoring network in a watershed. *Int J Environ Sci Technol* 11(2):303–310. <https://doi.org/10.1007/s13762-013-0195-2>
- Das S, Anandha Kumar KJ (2005) Management of Ground Water in Coastal Orissa, India. *Int J Ecol Environ Scie* 31(1):285–297
- De Montety V, Radakovitch O, Vallet-Coulomb C, Blavoux B, Hermitte D, Valles V (2008) Origin of groundwater salinity and hydrogeochemical processes in a confined coastal aquifer: case of the Rhône delta (Southern France). *Appl Geochem* 23(8):2337–2349
- Ekhmaj A, Ezlit Y, Elaalem M (2014) The situation of seawater intrusion in Tripoli, Libya. In *International Conference on Biological, Chemical and Environmental Sciences (BCES-2014)* June (pp. 14–15)
- ESA Land Cover CCI Product User Guide Version 2. Tech. Rep (2017) Available at: maps.elie.ucl.ac.be/CCI/viewer/download/ESACCI-LC-Ph2-PUGv2_2.0.pdf
- Fleury J (2005) PCA-CHEM new code using Matlab script for interpretative chemistry and microbiology data. *Matlab pour les nuls* no: 5
- Ganyaglo SY, Banoeng-Yakubo B, Osae S, Dampare SB, Fianko JR, Bhuiyan MA (2010) Hydrochemical and isotopic characterization of groundwaters in the eastern region of Ghana. *J Water Resour Protect* 2(3):199
- Gao Y, Qian H, Ren W, Wang H, Liu F, Yang F (2020) Hydrogeochemical characterization and quality assessment of groundwater based on integrated-weight water quality index in a concentrated urban area. *J Clean Prod* 260:121006. <https://doi.org/10.1016/j.jclepro.2020.121006>
- Gibbs RJ (1970) Mechanisms controlling world water chemistry. *Science* 17:1088–1090. <https://doi.org/10.1126/science.170.3962.1088>
- Gleeson T, Wada Y, Bierkens MF, Van Beek LP (2012) Water balance of global aquifers revealed by groundwater footprint. *Nature* 488(7410):197–200
- Gómez VMR, Gutiérrez M, Haro BN, López DN, Herrera MTA (2017) Groundwater quality impacted by land use/land cover change in a semiarid region of Mexico. *Groundw Sustain Dev* 5:160–167
- Goswami S, Rai AK (2022) Estimating suitability of groundwater for drinking and irrigation, in Odisha (India) by statistical and WQI methods. *Environ Monit Assess* 194(7):1–18
- Goswami S, Rai AK, Tripathy S (2022) Re-visiting Geothermal Fluid Circulation, Reservoir Depth and Temperature of Geothermal Springs of India. *J Hydrol* 612:128131
- Gupta PK (2002) Water and Energy Linkages for Groundwater Exploitation: A Case Study of Gujarat State, India. *Intl J Water Resour Dev* 18(1):25–45
- Hasan MSU, Rai AK (2020) Groundwater quality assessment in the Lower Ganga Basin using entropy information theory and GIS. *Journal of Cleaner Production*, 274, p.123077
- He S, Wu J (2019) Relationships of groundwater quality and associated health risks with land use/land cover patterns: a case study in a loess area, northwest China. *Human Ecol Risk Assess Intl J* 25(1–2):354–373
- Hem JD (1989) *Study and Interpretation of the Chemical Characteristics of Natural Water*. Water Supply Paper 2254, 3rd edition, US Geological Survey, Washington, DC, 263 pp
- Huang G, Liu C, Zhang Y, Chen Z (2020) Groundwater is important for the geochemical cycling of phosphorus in rapidly urbanized areas: a case study in the Pearl River Delta. *Environ Pollut* 260:114079. <https://doi.org/10.1016/j.envpol.2020.114079>
- Kelly W (2008) Long-term trends in chloride concentrations in shallow aquifers near Chicago. *Ground Water* 46:772–781. <https://doi.org/10.1111/j.1745-6584.2008.00466.x>
- Ketabchi H, Ataie-Ashtiani B (2015) Review: coastal groundwater optimization—advances, challenges, and practical solutions. *Hydrogeol J* 23(6):1129–1154
- Kundu N, Panigrahi M, Tripathy S, Munshi S, Powell M, Hart B (2001) Geochemical appraisal of fluoride contamination of groundwater in the Nayagarh District of Orissa, India. *Environ Geol* 41(3):451–460
- Larson TE, Buswell AM, Ludw HF, Langelier WF (1942) Calcium carbonate saturation index and alkalinity interpretations. *Journal (American Water Works Association)*, pp.1667–1684

- Li PY, Qian H, Wu JH, Ding J (2010) Geochemical modeling of groundwater in southern plain area of Pengyang County, Ningxia, China. *Water Sci Eng* 3(3):282–291
- Lobo-Ferreira JP, Chachadi AG, Diamantino C, Henriques MJ (2005) Assessing aquifer vulnerability to seawater intrusion using GALDIT Method. Part 1: application to the Portuguese aquifer of Monte Gordo
- Luszczynski NJ, Swarzenski WV (1996) Saltwater Encroachment in Southern Nassau and SE Queen Countries, Long Island, New York, USGS Paper, 1613-F
- MacQueen J (1967) Classification and analysis of multivariate observations. In 5th Berkeley Symp. Math. Statist. Probability, pp. 281–297
- Madhav S, Ahamad A, Kumar A, Kushawaha J, Singh P, Mishra PK (2018) Geochemical assessment of groundwater quality for its suitability for drinking and irrigation purpose in rural areas of Sant Ravidas Nagar (Bhadohi), Uttar Pradesh. *Geol Ecol Landscapes* 2:127–136. <https://doi.org/10.1080/24749508.2018.1452485>
- Manh DV, Van HV, Kien NC (2014) Evaluated saline intrusion west south coastline Vietnam. *J Marine Sci Technol Viet Nam* 14:217–234
- Manson SM, Burrough PA, McDonnell RA (1999) Principles of Geographical Information Systems: Spatial Information Systems and Geostatistics. *Econ Geogr* 75:422. <https://doi.org/10.2307/144481>
- Miller HJ, Han J (2009) Geographic data mining and knowledge discovery. CRC press
- Mohebbi MR, Saeedi R, Montazeri A, Vaghefi KA, Labbafi S, Okaie S, Abtahi M, Mohagheghian A (2013) Assessment of water quality in groundwater resources of Iran using a modified drinking water quality index (DWQI). *Ecol Indic* 30:28–34
- Mukherjee I, Singh UK, Singh RP (2021) An overview on heavy metal contamination of water system and sustainable approach for remediation. In: Singh A, Agrawal M, Agrawal SB (eds) *Water Pollution and Management Practices*. Springer Singapore, Singapore, pp 255–277. https://doi.org/10.1007/978-981-15-8358-2_11
- Nag SK, Das S (2017) Assessment of groundwater quality from Bankura I and II Blocks, Bankura District, West Bengal, India. *Appl Water Sci* 7. <https://doi.org/10.1007/s13201-017-0530-8>
- Naicker K, Cukrowska E, McCarthy TS (2003) Acid Mine Drainage Arising from Gold Mining Activity in Johannesburg, South Africa. *Environ Pollut* 122(1):29–40
- Nair AS, Indu J (2021) Assessment of groundwater sustainability and identifying factors inducing groundwater depletion in India. *Geophys Res Lett* 48(3):e2020GL087255
- Nayak P, Rai AK, Tripathy S (2017) Evaluating groundwater prospects using GIS techniques. *Sustain Water Resour Manage* 3(2):129–139
- Paliwal KV (1972) Irrigation with saline water, Monogram no. 2 (New series). New Delhi, IARI, 198
- Park SC, Yun ST, Chae GT, Yoo IS, Shin KS, Heo CH, Lee SK (2005) Regional hydrochemical study on salinization of coastal aquifers, western coastal area of South Korea. *J Hydrol* 313(3–4):182–194
- Raganath, H. M., (1987). *Groundwater* (2nd Edn.). Eastern Limited, New Delhi. pp. 344–369.
- Ranjan P, Wrat G, Bholia M, Mishra SK, Das J (2020Apr) A novel approach for the energy recovery and position control of a hybrid hydraulic excavator. *ISA Trans* 99:387–402. <https://doi.org/10.1016/j.isatra.2019.08.066>
- Rao NS, Dinakar A, Sravanthi M, Kumari BK (2021) Geochemical characteristics and quality of groundwater evaluation for drinking, irrigation, and industrial purposes from a part of hard rock aquifer of South India. *Environ Sci Pollut Res* 28(24):31941–31961
- Robson M, Spence K, Beech L (2006) Stream Quality in a Small Urbanised Catchment. *Sci Total Environ* 357(1–3):194–207
- Saaty TL (1980) The analytic hierarchy process: planning, priority setting, resource allocation. New York: McGraw 281
- Saha S, Reza AS, Roy MK (2019) Hydrochemical evaluation of groundwater quality of the Tista floodplain, Rangpur, Bangladesh. *Appl Water Sci* 9(8):1–12
- Sahu S, Gogoi U, Nayak NC (2021) Groundwater solute chemistry, hydrogeochemical processes and fluoride contamination in phreatic aquifer of Odisha, India. *Geosci Front* 12(3):101093
- Seifi A, Dehghani M, Singh VP (2020) Uncertainty analysis of water quality index (WQI) for groundwater quality evaluation: Application of Monte-Carlo method for weight allocation. *Ecological Indicators* 117:106653. <https://doi.org/10.1016/j.ecolind.2020.106653>
- Shannon CE, Weaver W (1947) The mathematical theory of communication. The University of Illinois Press, Urbana
- Shannon CE (1948) A Mathematical Theory of Communication. *Bell Syst Tech J* 27:623–656. <https://doi.org/10.1002/j.1538-7305.1948.tb00917.x>
- Shukla NK, Sahoo HK, Acharya S (2010) Assessment of groundwater quality of the coastal aquifers, north of Mahanadi River. *Environ Geochem* 12(1–2):1–10
- Sikdar PK, Chakraborty S (2008) Genesis of arsenic in groundwater of North Bengal Plain using PCA: a case study of English Bazar Block, Malda district, West Bengal, India. *Hydrol Process Intl J* 22(12):1796–1809
- Singh RP, Nath S, Prasad SC, Nema AK (2008) Selection of suitable aggregation function for estimation of aggregate pollution index for river Ganges in India. *J Environ Eng* 134(8):689–701
- Singh SK, Srivastava PK, Gupta M, Mukherjee S (2012) Modeling mineral phase change chemistry of groundwater in a rural-urban fringe. *Water Sci Technol* 66(7):1502
- Sophocleous M (2004) Global and regional water availability and demand: prospects for the future. *Nat Resour Res* 13(2):61–75
- Stoner JD (1978) Water-quality indices for specific water uses. Department of the Interior, Geological Survey
- Stumm W, Morgan JJ (2012) Aquatic chemistry: chemical equilibria and rates in natural waters (Vol. 126). John Wiley & Sons
- Sutadian AD, Muttill N, Yilmaz AG, Perera B (2016) Development of river water quality indices - a review. *Environ Monit Assess* 188:58–90
- Sutadian AD, Muttill N, Yilmaz AG, Perera BJC (2017) Using the Analytic Hierarchy Process to identify parameter weights for developing a water quality index. *Ecol Indic* 75:220–233
- Thapa R, Gupta S, Reddy DV et al (2017) An evaluation of irrigation water suitability in the Dwarka river basin through the use of GIS-based modeling. *Environ Earth Sci* 76:471. <https://doi.org/10.1007/s12665-017-6804-5>
- Tiwari AK, Singh AK (2014) Hydrogeochemical Investigation and Groundwater Quality Assessment of Pratapgarh District, Uttar Pradesh. *J Geol Soc Ind* 83:329–343
- Tiwari JN, Manzoor A (1988) Water quality index for Indian rivers. Ecology and pollution of Indian rivers. Aashish Publishing House, New Delhi, 271–286
- Ustaoglu F, Tepe Y, Taş B (2020) Assessment of stream quality and health risk in a subtropical Turkey river system: A combined approach using statistical analysis and water quality index. *Ecol Indic* 113:105815
- Walski TM, Parker FL (1974) Consumers water quality index. *J Environ Eng Div* 100:593–611
- Walton NRG (1989) Electrical Conductivity and Total Dissolved Solids—What is Their Precise Relationship? *Desalination* 72:275–292. [https://doi.org/10.1016/0011-9164\(89\)80012-8](https://doi.org/10.1016/0011-9164(89)80012-8)
- Watson DF (1992) *Contouring: A Guide to the Analysis and Display of Spatial Data: With Programs on Disket*. Pergamon, Oxford, 321

- Werner AD, Bakker M, Post VEA, Vandenbohede A, Lu C, Ataie-Ashtiani B, Simmons CT, Barry DA (2013) Seawater intrusion processes, investigation and management: Recent advances and future challenges. *Adv Water Resour* 51:3–26. <https://doi.org/10.1016/j.advwatres.2012.03.004>
- WHO (2017) Guidelines for Drinking-Water Quality: 4th Edition, Incorporating the 1st Addendum. World Health Organization, Geneva <http://apps.who.int/iris/bitstream/handle/10665/254637/9789241549950-eng.pdf?sequence=1>
- Williams LJ, Abdi H (2010) Principal component analysis. Wiley
- Interdisciplinary Reviews: Computational Statistics 2(4):433–459
- Xiao J, Wang L, Deng L, Jin Z (2019) Characteristics, sources, water quality and health risk assessment of trace elements in river water and well water in the Chinese Loess Plateau. *Sci Total Environ* 650:2004–2012

Publisher's note Springer Nature remains neutral with regard to jurisdictional claims in published maps and institutional affiliations.

Springer Nature or its licensor (e.g. a society or other partner) holds exclusive rights to this article under a publishing agreement with the author(s) or other rightsholder(s); author self-archiving of the accepted manuscript version of this article is solely governed by the terms of such publishing agreement and applicable law.